

NUMERICAL AND EXPERIMENTAL ANALYSIS OF POST-CRITICAL DEFORMATION STATES IN A TENSIONED PLATE WEAKENED BY A CRACK

TOMASZ KOPECKI

*Rzeszów University of Technology, Faculty of Mechanical Engineering and Aeronautics, Rzeszów,
Poland; e-mail: tkopecki@prz.edu.pl*

The paper presents the methodology of determination of the stress distribution in post-critical state of deformation of the rectangular plate weakened with the crack subjected to tension. The problem was formulated as physically and geometrically non-linear. Using the finite elements method, numerical analyses were performed. While solving the nonlinear issue, the progressive change of geometry of the structure in successive incremental steps were compared with results of experimental studies, performed simultaneously. The obtained results made the base for the assessment of reliability of effects of nonlinear numerical analysis, conditioned by the presence of imperfections of the plate in the neutral state. Two kinds of imperfections were considered: geometric - based on the assumption of the preliminary deflection of the plate in the zone of weakness and the second one – in form of load perturbation, normal to the middle surface of the plate.

Key words: plate, tension, crack, buckling, experiments, finite elements

1. Introduction

Rational approach to load-bearing structure design suggests necessity of focusing special attention on zones characterised with presence of high stress levels and gradients that are crucial for the structure durability and reliability. Determination of stress states in such zones in the design phase, when appropriate amendments can be introduced to the structure before time-consuming and expensive workshop prototype solution is realised, requires analysis of the structure performance within the full range of operationally permissible deformations. The above applies, in particular, to thin-walled structures in which post-critical deformation states occur within admissible load ranges. Solution

to the problem of stress distribution within these ranges requires application of nonlinear analysis based on numerical methods, mainly the finite element method. Despite the existence of a wide spectrum and algorithms useful in solving nonlinear problems, in the case of thin-walled structures with complex geometry, geometrical configurations corresponding to consecutive equilibrium states and obtained in the course of solving of a nonlinear problem can show significant divergence with respect to the current deformation state observed in the experiment.

Among that category of structures, one can count thin plates weakened by presence of cracks or cutouts. When such structures are subject to tensile stress in conditions of reaching or exceeding the critical load value, displacements in the direction normal to the plate plane known as wrinkling build up in the weakened zone appear and develop with the increasing load. The occurred post-critical deformation state results in fundamental change of plate geometry, a consequence of which redistribution of stress is significant.

As the cause of loss of stability of a plate weakened by e.g. a crack, the stress state arising as a consequence of tension can be considered. The state is characterised with presence of strong gradients, especially in the area adjacent to the crack front. That can be seen in an isochromatic fringe pattern observed in the plate model made of the optically active material (Fig. 1).

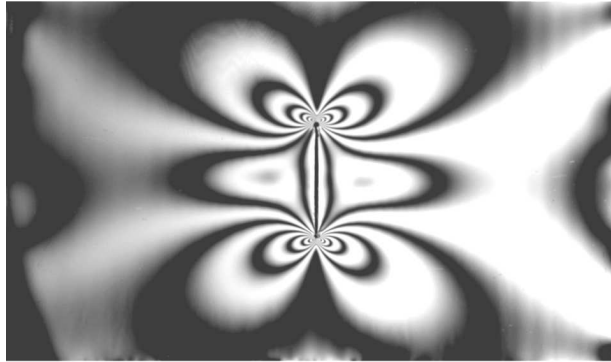


Fig. 1. Isochromatic fringe patterns in a tensioned plate with a crack

High orders of isochromatic fringes prove occurrence of high values of differences between main normal stresses with opposite signs. In the vicinity of the crack front, tensioning stresses occur oriented in the load direction together with high values of compression stress oriented transversally which, after reaching the critical load value, create favourable conditions for local buckling of the plate.

Problems concerning stability of rectangular plates subject to uniaxial tensile stress and weakened by presence of centrally located cracks were considered by many authors (Brighenti, 2005a,b; Dyshel, 2002; Markström and Storäkers, 1980; Riks *et al.*, 1992; Shaw and Huang, 1990; Sih and Lee, 1986). Those studies, carried out on the grounds of linearized theories, included mainly problems concerning determination of critical load values and plate buckling forms, depending on the orientation angle of the crack.

Striving to extend the scope of research of the wrinkling effect typical for thin-walled structures, in this paper one considered the problem consisting in determination of stress fields in advanced post-critical deformation states in a plate weakened by a crack. It was assumed that the problem was nonlinear in both physical and geometrical sense. One assumed as the postulate that for solving such a problem it is necessary to compare results of numerical analysis with appropriate results of experimental research. To this end, a plate of material showing elastic and inelastic properties was made, instantaneous characteristic of which was determined in an uniaxial tensile test. In the course of the experiment, the plate was subject to a variable load with a pulsating tensile force, as a result of which length of the crack increased, preserving its "natural" character of the defect. Numerical analysis was carried out for three selected crack lengths obtained in the course of fatigue tests, for which deformation distribution in the direction normal to the plate was recorded by means of the shadow moiré method (Patorski and Kujawińska, 1993).

Numerical calculations were carried out by means of the finite elements method. Emphasis was put on effectiveness of used methods and procedures ensuring conformity of calculation results with the experiment. The degree of deformation conformity in the post-critical state was adopted as a criterion of reliability of the stress state determined on the grounds of nonlinear numerical analysis (Crisfield, 1997; Felippa, 1976; Felippa *et al.*, 1994; *Theory...*, 2006).

2. Experimental research

The subject of the experiment consisted in a plate with dimensions 300 mm×250 mm, 0.7 mm thick (Fig. 2) made of polycarbonate with physical characteristics presented in Fig. 3.

In the central part of the plate, a crack was cut perpendicular to the load direction, with the initial length close to $L = 30$ mm. The full size of 30 mm was obtained as a result of propagation of the crack caused by a pulsating tensile load, varying from zero to $P_{max} = 1500$ N (Kopecki and Zacharzewski,

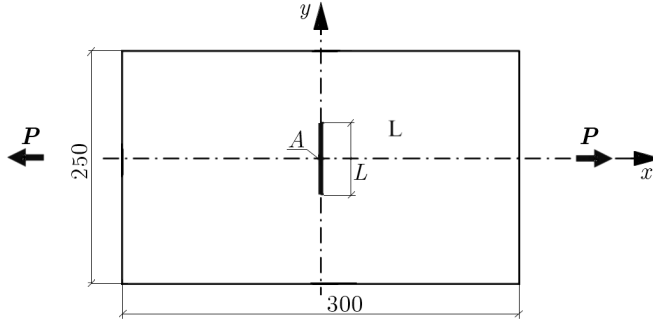


Fig. 2. Plate geometry

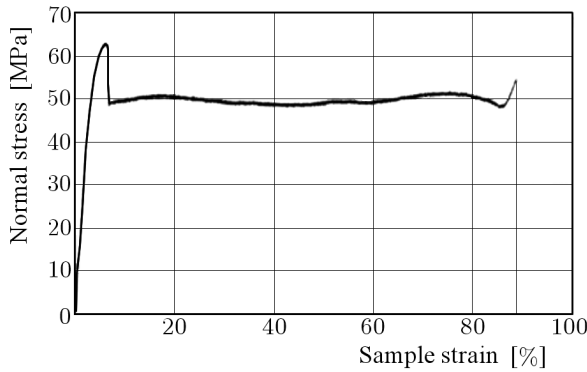


Fig. 3. Tensile stress-strain plot for the plate material

2006). The plate was mounted in the experimental set-up providing a constant pressure force of the clamps. This kind of mount provided homogeneity of the displacement field with the dominating component corresponding to the tensile force direction, outside the weakness zone, located in the vicinity of the crack. This homogeneity was monitored during the experiment by continuous observation in polarized light. Figure 4 shows the experimental set-up with the plated mounted.

As a result of variable load, length of the crack increased with the increasing number of load cycles. The experiment was carried out until the crack reached length of 70 mm.

Optical polarization properties of the plate material made possible simultaneous recording of optical phenomena occurring in circularly polarized light. The registration was carried out using the reflected light method. To this end, the inside surface of the plate was covered with a reflective layer. Figure 5 presents distribution of optical effects for three deformation states corresponding

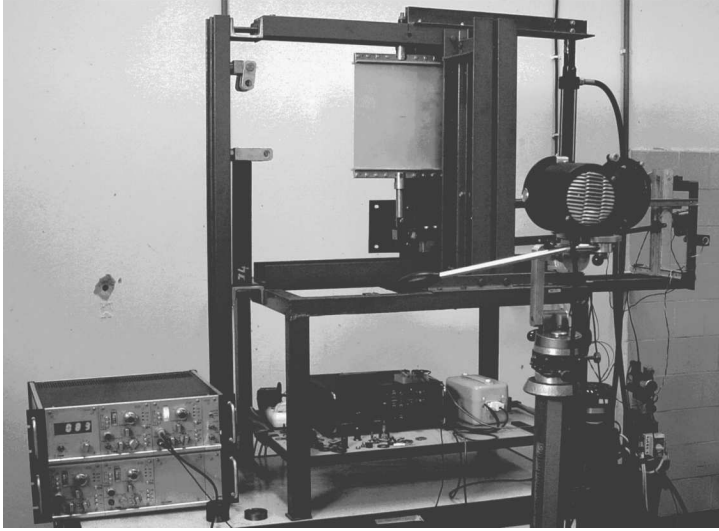


Fig. 4. The set-up for examination of crack propagation, isochromatic fringe patterns and transverse deformations by means of the moiré method

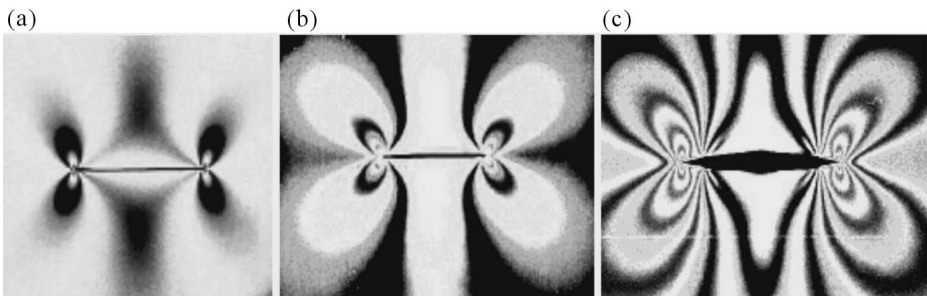


Fig. 5. Isochromatic fringe patterns in the crack zone at maximum load conditions; (a) $L = 30$ mm, (b) $L = 50$ mm, (c) $L = 70$ mm

to selected crack lengths. Recording of results was made at the same load level $P = 1500$ N.

The obtained patterns did not make a base for quantitative interpretation of the results because due to the presence of bending state in the zones of high effective stress levels, they cannot be interpreted as isochromatic lines (Aben, 1979; Laermann, 1982). Those patterns are very useful as qualitative experimental results for the assessment of the effective stress layouts obtained numerically and also for determination of load levels corresponding to first, local permanent deformations.

In each of the phases considered, deflection (displacement in the direction normal to the plate plane) was registered. A photograph depicting the post-critical deformation state corresponding to crack length $L = 70$ mm is presented in Fig. 6.

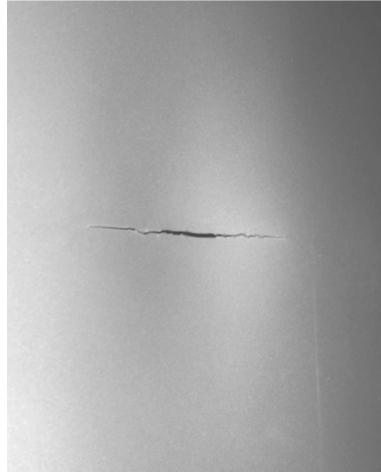


Fig. 6. Picture of plate wrinkling in the vicinity of crack with length $L = 70$ mm

The strain field recording was carried out by means of the shadow moiré method (Laermann, 1982). As a result, images of level contours were obtained (Fig. 7) corresponding to three selected plate weakening states.

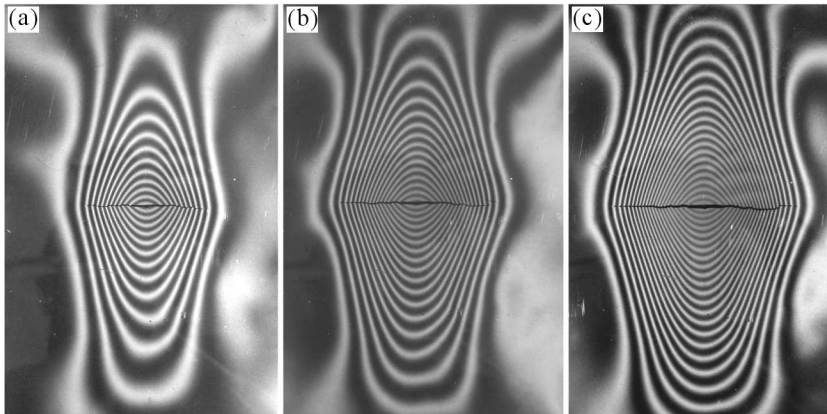


Fig. 7. Images of moiré fringes representing qualitative and quantitative nature of transverse deformations: (a) $L = 30$ mm, $f_{max} = 3.12$ mm, (b) $L = 50$ mm, $f_{max} = 4.42$ mm, (c) $L = 70$ mm, $f_{max} = 5.72$ mm

To each of the contours, a constant deflection corresponded. From selected raster parameters and image recording conditions, the distance between neighbouring contours was determined as equaling 0.26 mm. Thus, the maximum plate deflections in selected deformation phases were calculated (Fig. 7).

3. Numerical analysis

In nonlinear analysis of load-bearing structures, relations between a set of static parameters and corresponding set of geometric parameters can be presented in the form of a matrix equation (Aben, 1979; Felippa, 1976; Felippa *et al.*, 1994; Rakowski and Kacprzyk, 1993)

$$\mathbf{g} = \mathbf{K}^{-1}(\mathbf{g})\mathbf{f} \quad (3.1)$$

where \mathbf{g} is a set of geometric parameters describing the system deformation state caused by the load, \mathbf{f} is a set of static parameters, and \mathbf{K} is the stiffness matrix depending on the set of geometric parameters determining the current deformation state and a nonlinear constitutive relation.

In view of permanent deformations observed in the course of experiments, the plate material physical characteristics determined in the uniaxial tensile test (Fig. 3) was approximated by means of the ideally elastic-plastic body (Fig. 8).

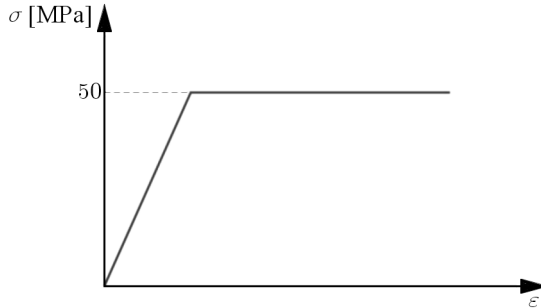


Fig. 8. The model of the material

In description of the constitutive equation related to the linear-elastic range

$$\boldsymbol{\sigma} = \mathbf{D}\boldsymbol{\varepsilon} \quad (3.2)$$

an assumption on the invariance of the normal segment ($\varepsilon_z = 0$) was kept in force. Therefore, the stress state in the plate is represented by vector $\boldsymbol{\sigma} = [\sigma_x, \sigma_y, \tau_{xy}, \tau_{yz}, \tau_{zx}]^\top$

$$\mathbf{D} = \frac{E}{1-\nu^2} \begin{bmatrix} 1 & \nu & 0 & 0 & 0 \\ \nu & 1 & 0 & 0 & 0 \\ 0 & 0 & \frac{1-\nu}{2} & 0 & 0 \\ 0 & 0 & 0 & \frac{1-\nu}{2k} & 0 \\ 0 & 0 & 0 & 0 & \frac{1-\nu}{2k} \end{bmatrix} \quad (3.3)$$

is the material constants matrix in which the effect of non-dilatational strain on the plate elastic energy was accounted for by introducing a correction coefficient $k = 1.2$ (*Theory...*, 2006), while

$$\boldsymbol{\varepsilon} = \begin{bmatrix} \varepsilon_x \\ \varepsilon_y \\ \gamma_{xy} \\ \gamma_{yz} \\ \gamma_{zx} \end{bmatrix} = \begin{bmatrix} \frac{\partial u}{\partial x} + \frac{1}{2} \left[\left(\frac{\partial u}{\partial x} \right)^2 + \left(\frac{\partial v}{\partial x} \right)^2 + \left(\frac{\partial w}{\partial x} \right)^2 \right] \\ \frac{\partial v}{\partial y} + \frac{1}{2} \left[\left(\frac{\partial u}{\partial y} \right)^2 + \left(\frac{\partial v}{\partial y} \right)^2 + \left(\frac{\partial w}{\partial y} \right)^2 \right] \\ \frac{\partial u}{\partial y} + \frac{\partial v}{\partial x} + \frac{\partial u}{\partial x} \frac{\partial u}{\partial y} + \frac{\partial v}{\partial x} \frac{\partial v}{\partial y} + \frac{\partial w}{\partial x} \frac{\partial w}{\partial y} \\ \frac{\partial u}{\partial z} + \frac{\partial w}{\partial y} + \frac{\partial u}{\partial y} \frac{\partial u}{\partial z} + \frac{\partial v}{\partial y} \frac{\partial v}{\partial z} + \frac{\partial w}{\partial y} \frac{\partial w}{\partial z} \\ \frac{\partial u}{\partial z} + \frac{\partial w}{\partial x} + \frac{\partial u}{\partial x} \frac{\partial u}{\partial z} + \frac{\partial v}{\partial x} \frac{\partial v}{\partial z} + \frac{\partial w}{\partial x} \frac{\partial w}{\partial z} \end{bmatrix} \quad (3.4)$$

is a vector containing deformation state components corresponding to the Green-Saint-Venant deformation tensor (*Theory...*, 2006), and u , v , w are displacement vector components in local system of coordinates x , y , z .

Numerical representations of the system nonlinear deformations are based on the assumption that at any solution stage with the corresponding load, the deformed system retains always a static equilibrium state. Thus, for a defined discrete system it is possible to formulate a system of equilibrium equations that, with respect to nonlinear structural analysis in its displacement-based representation, can be expressed in form of the residual force matrix equation:

$$\mathbf{r}(\mathbf{u}, \boldsymbol{\Lambda}) = \mathbf{0} \quad (3.5)$$

where \mathbf{u} is the state vector containing displacement components of the structure nodes corresponding to the current geometrical configuration, $\boldsymbol{\Lambda}$ is the matrix composed of control parameters corresponding to the current load state, and \mathbf{r} is the residual vector containing uncompensated components of forces related to the current system deformation state (Crisfield, 1997; Felippa *et al.*, 1976).

In numerical algorithms, the components of matrix $\boldsymbol{\Lambda}$ are expressed as functions of the parameter λ defined as the state control parameter. It is

a measure of increase of load related indirectly or directly with the pseudo-time parameter t . Thus, the system of equilibrium equations (3.5) can be also presented in the form

$$\mathbf{r}(\mathbf{u}, \lambda) = \mathbf{0} \quad (3.6)$$

The above equation is known as a monoperametric residual force equation. Its solution includes a finite number of consecutive structure deformation states, while each state corresponds to a combination of varying control parameters related to the system load, expressed by a single state control parameter λ . Transition from the current state to the subsequent one, representing the incremental step, is initialized by change of the control parameter related to new structure geometry determined by the new state vector (Felippa, 1976; Ramm, 1982).

Development of numerical methods reflected in contemporary algorithms used in professional commercial programs resulted in constitution of their two fundamental types. The first one includes purely incremental methods known also as prediction ones, while the other type encompasses correction methods, called also prediction-correction or incremental-iteration methods. The first of the mentioned groups is characterised with limited, often unsatisfactory accuracy of obtained results. Moreover, they exclude continuation of calculations after crossing critical points on the equilibrium path. Introduction of the iteration phase is therefore aimed at reduction of the solution error and possibility to determine critical points. That makes possible to analyse the structure in advanced deformation states.

A feature common for both method types consists in presence of the incremental phase. With respect to arbitrary increment, at transition from n -th to $(n + 1)$ -th state, the undetermined quantities are

$$\Delta \mathbf{u}_n = \mathbf{u}_{n+1} - \mathbf{u}_n \quad \Delta \lambda_n = \lambda_{n+1} - \lambda_n \quad (3.7)$$

In order to determine them, an additional incremental control equation is formulated, known as the equation of constraints, expressed in form of the condition

$$c(\Delta \mathbf{u}_n, \Delta \lambda_n) = 0 \quad (3.8)$$

The fundamental component of the incremental phase is its prediction step, determining a point in the state hyperspace corresponding to the subsequent state configuration defined by determination of the increment $\Delta \mathbf{u}$ for the assumed $\Delta \lambda$ with equation (3.8) satisfied as the same time. Error of the solution at each increment step depends on the increment control equation and the adopted extrapolation formula. In each consecutive increment step, the value of

total error may increase, resulting in occurrence of the so-called drift error. Its minimization is ensured by the iteration phase.

The fundamental method used in solution of structural mechanics nonlinear problems is the Newton-Raphson method with numerous program realisations and variations constituting a whole family of methods (Crisfield, 1997; Felippa *et al.*, 1994; Rakowski and Kacprzyk, 1993). The core idea of these methods consists in expansion of the residual forces equation $\mathbf{r} = \mathbf{0}$, and the increment control equation $c = 0$, into Fourier series.

Assuming that, as a result of k -th correction iteration step, values \mathbf{u}^k and λ^k are obtained and the equations take the following forms

$$\begin{aligned} \mathbf{r}^{k+1} &= \mathbf{r}^k + \frac{\partial \mathbf{r}}{\partial \mathbf{u}} \mathbf{d} + \frac{\partial \mathbf{r}}{\partial \lambda} \eta + \beta = \mathbf{0} \\ c^{k+1} &= c^k + \frac{\partial c}{\partial \mathbf{u}} \mathbf{d} + \frac{\partial c}{\partial \lambda} \eta + \beta = 0 \end{aligned} \quad (3.9)$$

where

$$\mathbf{d} = \mathbf{u}^{k+1} - \mathbf{u}^k \quad \eta = \lambda^{k+1} - \lambda^k \quad (3.10)$$

Terms β in both equations include neglected residual values of higher orders. In the iteration process, consecutive values \mathbf{d} and η are determined with respect to which the solution convergence condition is checked at the assumed tolerance. The resulting set constituting a solution to nonlinear algebraic equations with respect to unknown nodal displacements, creates a base for determination of the equilibrium path. The path, representing a relation between the static parameters corresponding to the structure and geometrical parameters related to displacements of its individual points represents a hyper-surface in a multidimensional space with the number of dimensions corresponding to the number of degrees of freedom of the system taken into account. In practice, representative relations between the two parameters are usually developed.

As a representative relation for determination of the equilibrium path in the problem considered herein, a functional dependence between the maximum deflection value at the crack half-length and the plate tensioning force is assumed.

As a base in search for the solution, the incremental Newton-Raphson method and correction strategy based on the arc length control concept in the Riks-Wempner approach was adopted (Ramm, 1982). Attempts to use only the Newton-Raphson methods led to excessive divergence between the results of numerical calculations and the experiment as for the geometry of occurring wrinkling. The reliability of obtained results was assessed by comparing both equilibrium path shapes and deformation geometries. The two elements

created a base for repeated corrections of the numerical model (Kopecki and Dębski, 2007).

The plate was modelled using a curved four-node thin-shell element. It is an isoparametric double curved element described by means of bicubic interpolation functions, based on the Koiter-Sanders shell theory (*Theory...*, 2006). At each node, the element has the following 12 degrees of freedom

$$u, \frac{\partial u}{\partial \theta^1}, \frac{\partial u}{\partial \theta^2}, v, \frac{\partial v}{\partial \theta^1}, \frac{\partial v}{\partial \theta^2}, w, \frac{\partial w}{\partial \theta^1}, \frac{\partial w}{\partial \theta^2}, \frac{\partial^2 u}{\partial \theta^1 \partial \theta^2}, \frac{\partial^2 v}{\partial \theta^1 \partial \theta^2}, \frac{\partial^2 w}{\partial \theta^1 \partial \theta^2}$$

where (θ^1, θ^2) are Gaussian coordinates related to the shell central plane, u, v, w are displacement components defined in global Cartesian system of coordinates x, y, z . Analysis of large deformations is ensured by use of Lagrange approximation functions. That approximation includes also the variant with finite deflections and torsions, with the assumption on small deformation tensor remaining in force. Use of such an element is recommended in nonlinear analysis of thin-walled structures (*Theory...*, 2006).

A number of conditions related to the approximate nature of finite element method, distinguishing the resulting numerical solutions from the exact ones based on continuous medium models result in the fact that the obtained results are, by their nature, charged with a solution error or, more precisely, with a discretization error. The discretized solution tends to the strict one, when the characteristic length of the used finite element tends to zero. That means in fact that numerical solving of a problem should be performed many times, "improving" consecutive results. That common practice, in case of nonlinear analysis, sometimes encounters difficulties of both software and hardware nature. They are especially evident in analysis of thin-walled structures.

For instance, a plate with a crack in its area but having no geometric imperfection in the direction normal to its plane, when subject to nonlinear numerical analysis should not, by assumption, lead to any deformation in the normal direction. Complexity of the numerical procedure, as well as hardware-related conditions, may sometimes lead to results suggesting correctness of the obtained solution.

3.1. Plate without imperfection

Real mechanical systems are characterised by the presence of various inaccuracies, which can be connected with not ideal geometry of objects or their material and load faults. This inaccuracies are widely called imperfections. A significance of kinds and values of imperfections will be considered in detail, using an example of the considered plate.

The numerical model of the plate containing a crack in its area, without any imperfection, analysed using a nonlinear procedure, according to principles should not have any displacements in the direction normal to the plain of the plate. However, the complexity of nonlinear procedures and numerical factors can lead to results suggesting the correctness of the incorrect solution.

In order to provide a quantitative example for illustration of the issue of divergence of results with respect to the obtained ones, a numerical analysis was carried out based on the plate geometry according to Fig. 2 with the crack of length $L = 30$ mm. An ideal elastic-plastic material physical characteristics were adopted (Fig. 3): $\text{Re} = 50$ MPa, $E = 3000$ MPa, $\nu = 0.36$, and the load in form of evenly distributed tensile forces applied to the plate shorter edges. Along the longer edges, the degree of freedom was blocked corresponding to translation in the direction perpendicular to the plate plane. Moreover, displacements along the load direction were constrained in two nodes located on the plate longer edges, on its transverse symmetry axis. The nonlinear analysis was carried out by means of MSC-Marc-7 software and MSC-Patran pre- and postprocessor. As a result, in the zone adjacent to the crack, a symmetric form of transversal deformation was obtained shown in form of contours in Fig. 9.

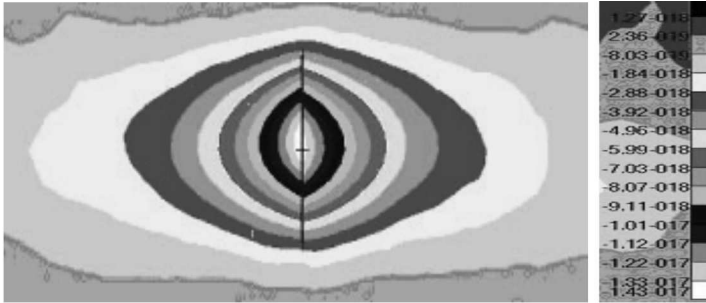


Fig. 9. Constant deflection value (in cm) contours in the crack zone for the plate without imperfection. A model based on regular mesh (12 700 elements)

Despite geometrical similarity of constant deflection contour patterns, the results, from the quantitative point of view, do not reflect the deformation state identified in the experiment. What attracts attention is negligibly small absolute maximum value of the deflection equaling $1.43 \cdot 10^{-17}$ cm. Similar results were obtained no matter what parameters controlling the course of analysis, increment method or correction strategy was adopted. In Fig. 10, the distribution of effective stress according to H-M-H hypothesis is presented.

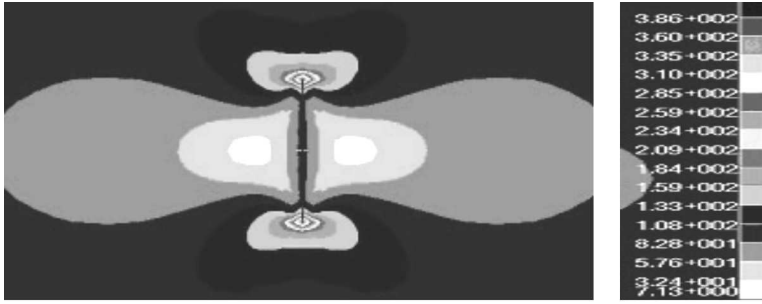


Fig. 10. Contours representing equivalent stress distribution according to H-M-H hypothesis. The plate without imperfection $\sigma_{max} = 36.8$ MPa

The maximum effective stress value amounted to 36.8 MPa which means that under the load of tensile force $P_{max} = 1500$ N, no non-elastic deformation occurred. The result is inconsistent with the outcome of the experiment that showed presence of permanent deformation after load release. It can be thus concluded that attempts to solve the problem of the flat plate without imperfection weakened by presence of a crack as a geometrically nonlinear problem leads to incorrect results with an understated equivalent stress level.

3.2. Plate with geometric imperfection

In the light of results presented above, in the next step of discussion a geometrical imperfection of the plate was taken into account. It consisted in placement of a centrally located point A (Fig. 2) outside the plate plane in the normal direction. To determine the order of magnitude of the introduced defect in neutral state, a number of preliminary analyses was carried out in which a number of its different values was assumed. Finally, numerical analysis was carried out with an initial deflection value at point A equaling 1 mm. A number of mesh variants was considered. As a basic one, an irregular mesh was adopted, concentrated in the zone adjacent to the crack. The regular mesh option was also taken into account. In both cases, the number of elements did not exceed 13 000. The presence of a crack was modelled by introducing doubled nodes with the same coordinates, assigned symmetrically to two adjacent areas on both sides of the crack edge. Identical model fastening and loading scheme was used as in the case of the plate without imperfection.

Calculations were carried out by means of MSC-Marc-7 program, offering possibility to choose parameters of nonlinear analysis and select among different incremental methods and correction strategies.

In the course of preliminary analyses, a number of cases were encountered resulting, as it can be assumed, partly from geometrical conditions and partly from (not very fortunate) the initial selection of control parameters for calculation procedures, in which in the course of one of consecutive incremental steps the rapid change of sign of the control parameter into negative occurred. One such a case was observed in the course of analysis based on a regular mesh and using the Newton-Raphson method (Rakowski and Kacprzyk, 1993) with a correction strategy corresponding to the Riks-Ramm arc length control method (Ramm, 1982). As a result of the above-mentioned control parameter sign change, a "turn-up" of shorter loaded edges of the plate beyond its plane occurred.

Causes of similar incorrect results can be sought in too large system stiffness increase in consecutive steps and the resulting possibility of occurrence of a turning point on the equilibrium path. It was found that effective methods of elimination of the obtained irregularity are: change of the increment method and/or correction strategy. In the problem considered herein, a fundamental solution quality improvement (at minimum correction of control parameters) was obtained by replacing the Newton-Raphson algorithm with the secant method, and switching at the same time from the arc length correction to the hyperspherical Crisfield correction method (Crisfield, 1997; Ramm, 1982). Consequently, a solution was obtained in which the deflection distribution in the vicinity of the crack (Fig. 13) turned out to be consistent in its character with that obtained experimentally (Fig. 7a).

As a result, in the vicinity of the crack, a deflection distribution presented in Fig. 11 was obtained.

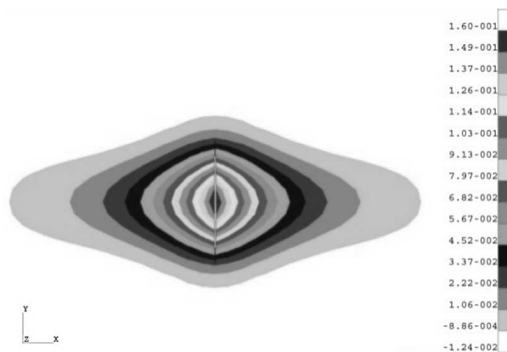


Fig. 11. Plate deflection contours in the vicinity of the crack with length $L = 30$ mm. Model based on regular mesh with geometric imperfection (in cm)

In the case of irregular mesh being used, with the same numerical procedures and identical set of control parameters, a similar result was obtained, shown in Fig. 12.

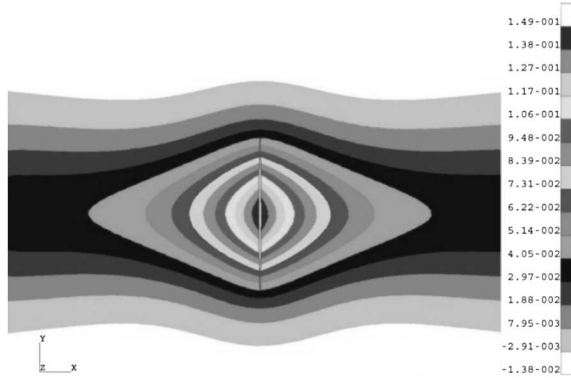


Fig. 12. Deflection contours in the vicinity of the crack with length $L = 30$ mm. Model with geometric imperfection based on irregular mesh

Restricting ourselves to comparative assessment of the presented calculation results with results of the experiment (Fig. 7a), we can conclude that for both mesh variants the obtained results show satisfactory conformance as far as deflection distributions are concerned. However, quantitative comparison reveals divergence between the calculation and experimental results. A numerical manifestation of that divergence are maximum values of calculated deflections amounting to about 80% of actual values. Calculations performed for the plate with a crack 50 mm long demonstrated slightly better convergence of the maximum deflection with the experiment exceeding 80% by a little. A fundamental change was obtained for a crack with length of 70 mm. Here, conformity was as high as 95%. As formality, it must be mentioned that numerical values of deflection obtained as a result of numerical analysis represent deflection increments above the initial value resulting from the assumed imperfection, while the results of the experiment carried out by means of the moiré method represent actual deflection magnitudes.

In Fig. 13, plate deflection patterns for cases where the crack reached length of 50 mm and 70 mm, respectively, are presented in form of level contours. In both cases, the same geometric imperfection was assumed consisting in placement of point A (Fig. 2) outside the plate plane at a distance of 1 mm.

In Figs. 14, 15 and 16, equivalent stress distribution patterns are presented according to H-M-H hypothesis corresponding to calculated deformations. By comparing the results, it can be concluded that differences in the maximum

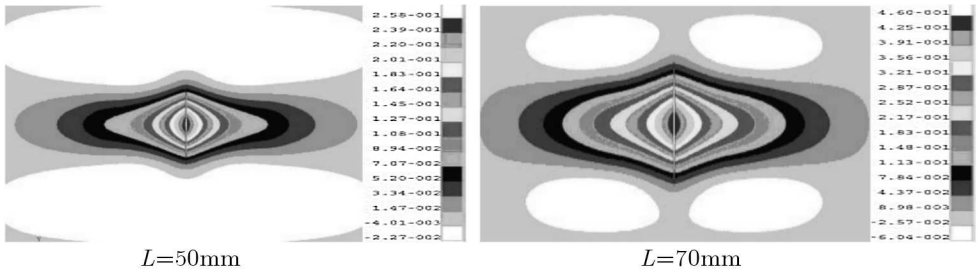


Fig. 13. Deflection contours in the vicinity of the crack in models with irregular mesh

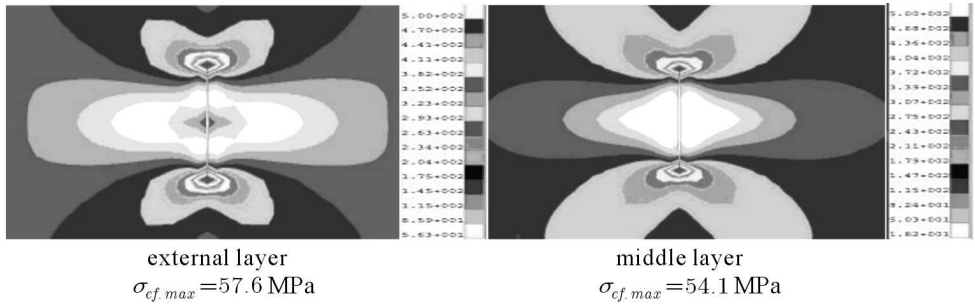


Fig. 14. Equivalent stress distribution according to H-M-H hypothesis in the vicinity of the crack with length $L = 30$ mm in the plate model with irregular mesh and geometric imperfection

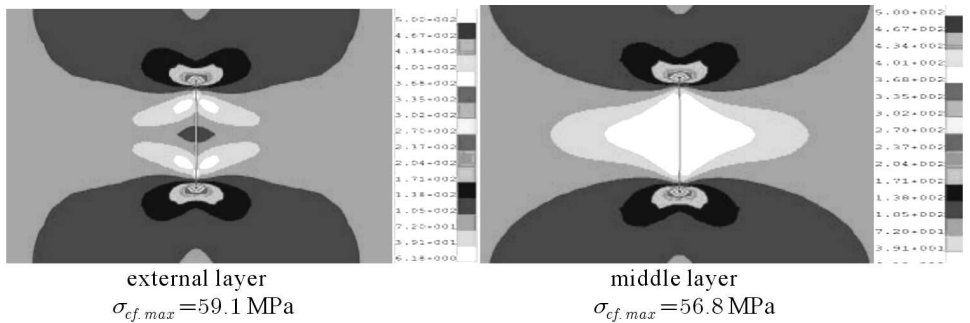


Fig. 15. Equivalent stress distribution according to H-M-H hypothesis in the vicinity of the crack with length $L = 50$ mm in the plate model with irregular mesh and geometric imperfection

values of reduced stresses, accounting for the flexural and membrane stress state, in the crack front zone, in both middle and external layer, are larger in the case of cracks with smaller lengths. As the crack length increases, the plasticization zone becomes virtually homogeneous along the plate thickness. In the most advanced deformation phase, deflection gradients also decreased,

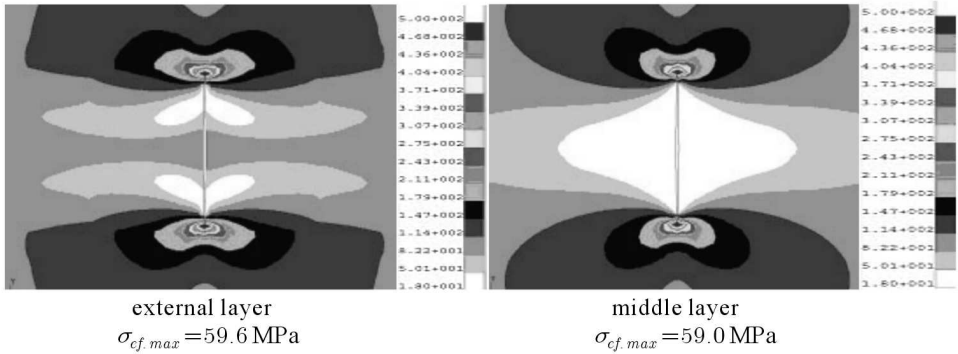


Fig. 16. Equivalent stress distribution according to H-M-H hypothesis in the vicinity of the crack with length $L = 70 \text{ mm}$ in the plate model with irregular mesh and geometric imperfection

which shows that as crack length increases, the membrane state becomes the dominant one.

In order to determine to what extent the conformance of deformations obtained from numerical calculations and from the experiment depends on the value of imposed imperfection, a number of numerical tests was carried out. They have shown that with increasing preliminary deflection above 1 mm, the divergence of results in the wrinkling increases with respect to both values and deformation character. The effect is confirmed by calculation results presented in Fig. 17.

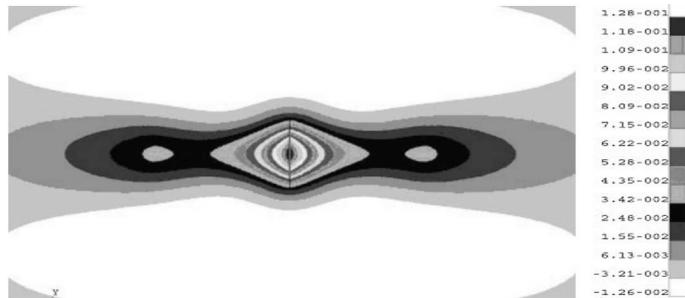


Fig. 17. Displacement distribution in the model with irregular mesh and geometric imperfection increased to 1.5 mm; $L = 30 \text{ mm}$

In that case, calculations were based on the model with an irregular mesh and geometric imperfection of 1.5 mm, representing 48% of the maximum deflection value obtained experimentally. The maximum value of calculated deflection amounting to 2.78 mm turned out to be 89% of the value observed in the experiment. Moreover, the distribution of contours (Fig. 17) shows that the case appears the most divergent one.

The performed tests and analyses allow one to conclude that the precondition of rational determination of the stress field in a weakened flat structure using exclusively nonlinear numerical analysis consists in introduction of such an imperfection that would ensure representation of the object geometry in the post-critical state remaining in as good conformity with results of experiment as possible.

3.3. Imperfection imposed by means of load normal to plate plane

As an alternative to geometric imperfection, an idea was considered consisting in introduction, for the ideally flat structure, of a small transversal perturbation, non-negligible in nonlinear static numerical analysis. The simplest method of realisation of a defect of that kind consisted in loading the plate with a discrete normal force, localised at the central point A at the crack half-length. Preliminary analyses revealed that such a method led to significant variance of calculation results with respect to those observed in the experiment. What proved to be effective instead was the application of continuous transverse load with constant intensity along both edges of the crack and less by several orders of magnitude with respect to the plate load force (Fig. 18).

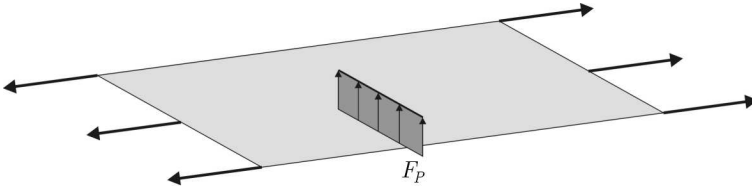


Fig. 18. Method of introduction of a perturbation initializing transversal deformation of the plate

The method was used in nonlinear analyses of identical models that were considered when a geometric imperfection was used. Load values were selected in a way ensuring the best possible conformance of plate deflection fields obtained numerically and experimentally. As a criterion, the maximum deflection values were adopted and similarity of contours representing constant deflection values. The best convergence of results was obtained using the secant increment method, combined with the Riks-Ramm arc length control or Crisfield hyperspherical control correction strategy.

The plot presented in Fig. 19 shows the relation between crack length and magnitude of total transverse load F_P (Fig. 18) ensuring a satisfactory conformance of the calculation results with the experiment.

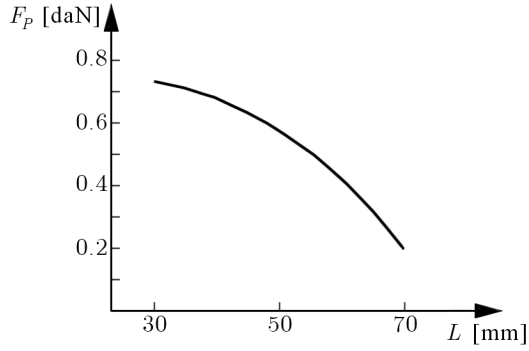


Fig. 19. Transverse load applied to the crack edge vs. crack length

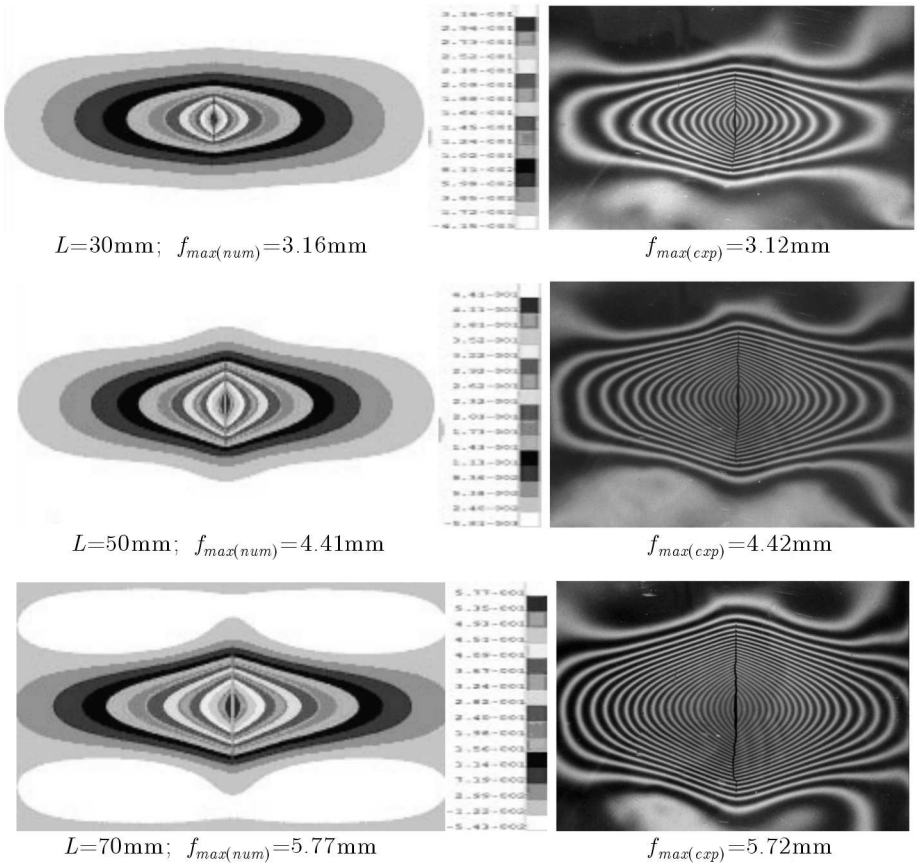


Fig. 20. Comparison of deflection distributions in the post-critical state. Models with continuous normal load

Figure 20 shows deflection distributions in the post-critical state in the plate subject to the test for three crack lengths values: 30 mm, 50 mm, 70 mm, for the identical load with a tensile force of 1500 N. The fact worth of attention consists in almost perfect conformity of deflection values obtained as a result of numerical analysis $f_{max(num)}$, and in the experiment $f_{max(exp)}$.

Results presented in Fig. 20 prove the existence of a satisfactory similarity of contours representing constant deflection values obtained by means of numerical calculations and observed in the experiment. They make a base for a conclusion that, according to the solution uniqueness rule, stress fields corresponding to the considered deformation states and determined by means of numerical analysis remain in conformity with the state occurring in the actual structure.

Figure 21 presents equivalent stress distributions according to H-M-H hypothesis in the middle and external layer, corresponding to deformations shown in Fig. 20.

Equivalent stress distributions show that with increasing crack length, differences in the stress distributions in the central and external surface disappear.

In view of dominance of the membrane state in conditions of advanced deformations, the observed optical effects can be interpreted as "pure" isochromatic, not disturbed by the flexural state.

In Fig. 23, representative equilibrium paths are presented for numerical models with geometric imperfections and models with an imperfection imposed by means of the initial normal load. They represent relations between the maximum deflection value (at the crack half-length) and the resultant tensile force.

The presented equilibrium paths for both forms of the imposed imperfection, although similar as for the nature of the phenomenon, are quantitatively different. The results based on imposition of geometric imperfection led to overestimated plate stiffness.

4. Conclusions

Nonlinear numerical analyses and experimental test carried out suggest a number of conclusions that seem to be interesting from the research point of view.

An observation of fundamental importance consists in the fact that – according to the experimental research – transition of the structure under examination to the post-critical deformation state occurs smoothly, simply difficult to

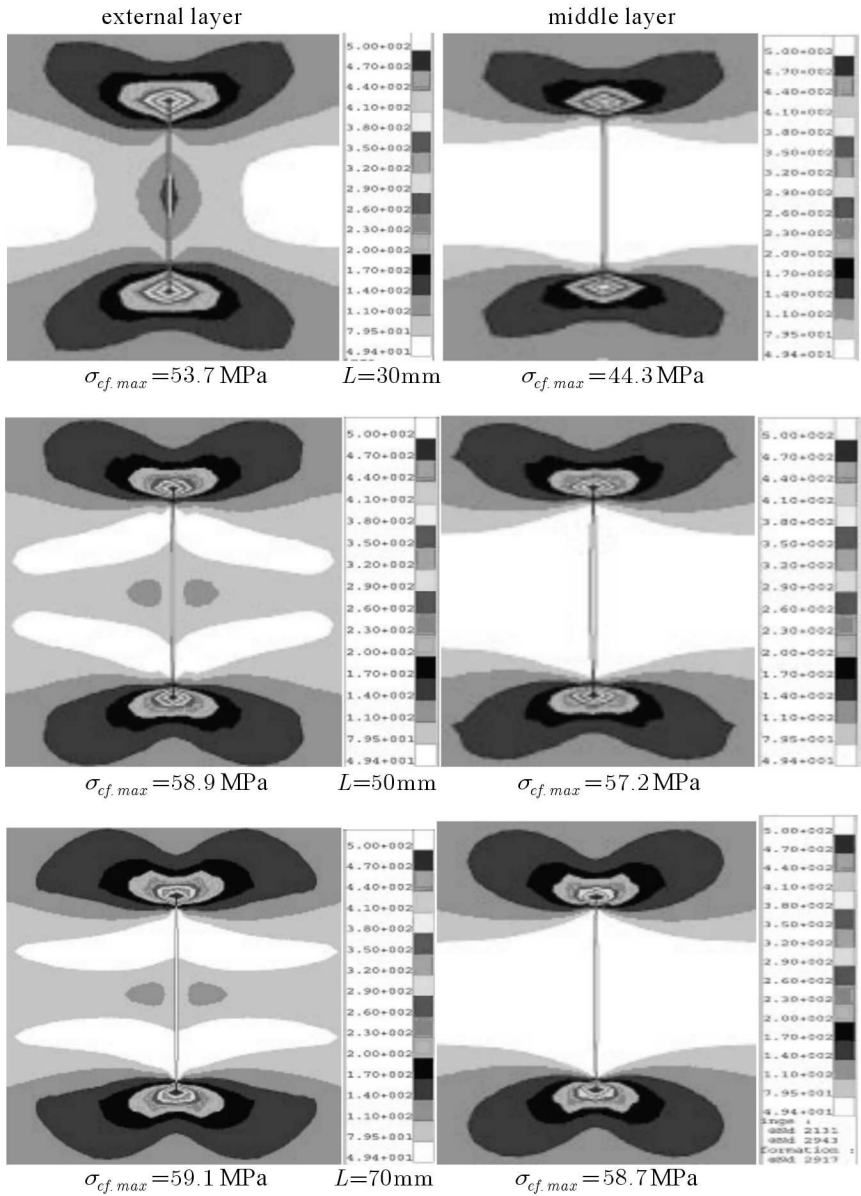


Fig. 21. Equivalent stress distribution according to H-M-H hypothesis in the crack front zone. Models with continuous normal load in the neutral state

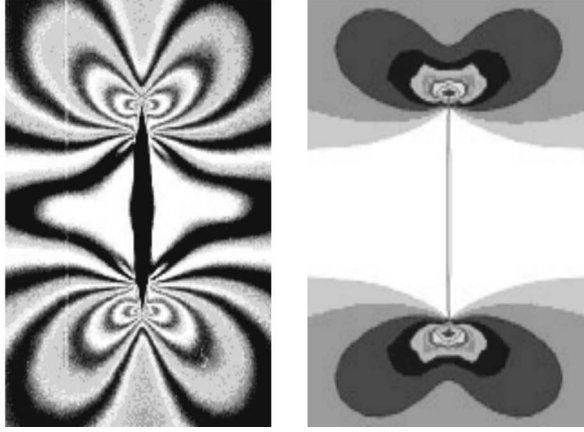


Fig. 22. Similarity of isochromatic fringe patterns with the equivalent stress distribution according to τ_{max} hypothesis in the central surface ($L = 70$ mm)

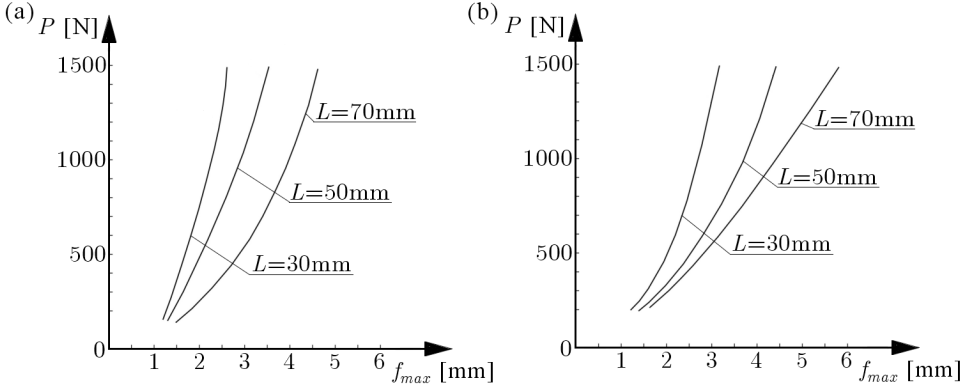


Fig. 23. Equilibrium paths showing load vs. maximum deflection; (a) models with geometric imperfection, (b) models with imperfection imposed by a load

notice, despite the use of the deflection measurement method with sufficiently high sensibility for that kind of a task.

Relations: the cause (tensile force) vs. the effect (maximum deflection value), constituting the parameters of representative equilibrium path (Fig. 26) reveal the nonlinear nature of phenomena occurring for both types of imposed imperfections. They are similar as for the nature of nonlinearity, but differ with respect to their values.

Results of calculations based on the geometric imperfection imposition concept lead to overstated stiffness of the structure, as a result of which they do not assure satisfactory conformity with the experiment.

An important element among the discerned relations is the conformity of the equilibrium path obtained as a result of numerical calculation and, presented in Fig. 25, from the experiment. The experimental path was developed on the grounds of deflection level contours recorded in the course of examination of the crack with length of 30 mm at three load levels: 500 N, 1000 N and 1500 N (Fig. 24).

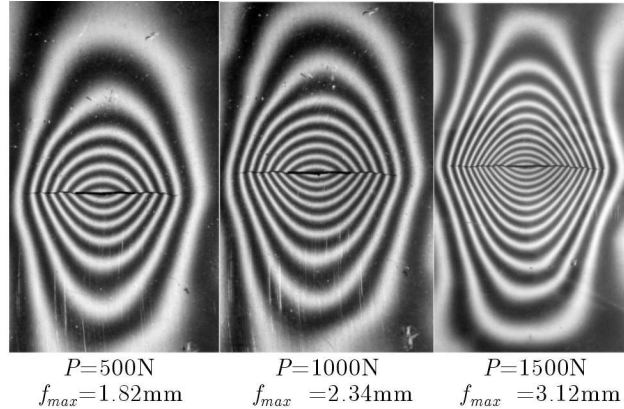


Fig. 24. Deflection level contours for a constant crack length $L = 30$ mm

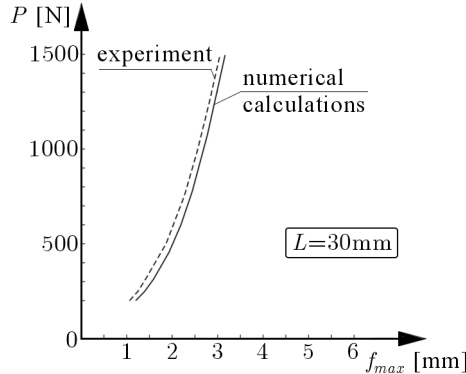


Fig. 25. Equilibrium paths for a crack with length $L = 30$ mm

It can be concluded on the grounds of the above analysis that introduction of a perturbation in form of a continuous normal load in the weakening zone is a definitely more rational method of numerical representation of the effect of wrinkling of plates with cracks, assuring both qualitative and quantitative conformity with actual deformation of the structure. However, the method requires a proper selection of the load value, resulting in advisability, and sometimes necessity to carry out an experiment of local nature.

The presented methodology seems to be applicable with satisfactory results to flat structures with discontinuities of other kinds. Such a suggestion follows from preliminary studies on crack propagation initiated in a plate with a circular cutout (Fig. 26).

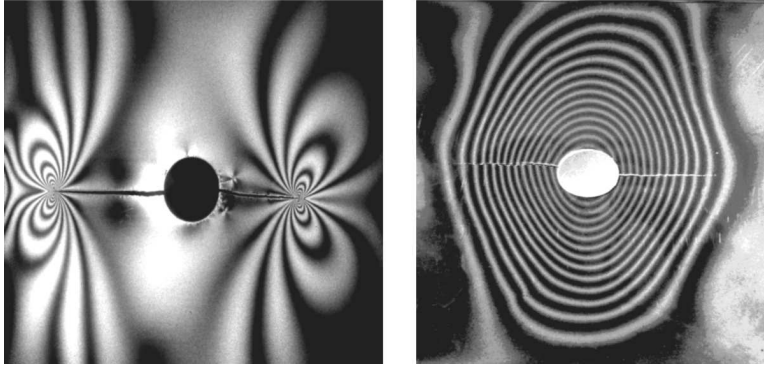


Fig. 26. Pictures of the wrinkling effect in a plate with a circular cutout subject to fatigue tests

In view of increasing possibilities in computer coding of nonlinear characteristics of material models, including optically active ones, realisation of an adequate experiment can be significantly supported by theoretical research, serving as the base for determination of efficiency of both developed numerical model and adopted procedure.

Transfer of results onto real objects made of other materials with physical characteristics that could be approximated by means of the perfect elastic-plastic body can be reduced to determination of material constants entered into the calculation code or it becomes possible on the grounds of model similarity.

References

1. ABEN H., 1979, *Integrated Photoelasticity*, McGraw-Hill Book Co., London
2. BRIGHENTI R., 2005a, Buckling of cracked thin-plates under tension and compression, *Thin-Walled Structures*, **43**, 209-224
3. BRIGHENTI R., 2005b, Numerical buckling analysis of compressed or tensioned cracked thin plates, *Eng. Struct.*, **27**, 265-276

4. CRISFIELD M.A., 1997, *Non-Linear Finite Element Analysis of Solids and Structures*, J.Wiley & Sons, New York
5. DYSHEL M.S., 2002, Stability and fracture of plates with a central and an edge crack under tension, *Int. Appl. Mech.*, **38**, 472-476
6. FELIPPA C.A., 1976, *Procedures for Computer Analysis of Large Nonlinear Structural System in Large Engineering Systems*, A. Wexler (Edit.), Pergamon Press, London
7. FELIPPA C.A., CRIVELLI L.A., HAUGEN B., 1994, A survey of the core-congruential formulation for nonlinear finite element, *Arch. of Comput. Meth. in Enging.*, **1**
8. KOPECKI T., DĘBSKI H., 2007, Buckling and post-buckling study of open section cylindrical shells subjected to constrained torsion, *Arch. of Mech. Enging.*, **LIV**, 4
9. KOPECKI T., ZACHARZEWSKI J., 2006, Fatigue life and stress state analysis of cracked thin-walled plate under cycles axial tension, *Maintenance and Reliability*, **31**, 3, 19-26
10. LAERMANN K.H., 1982, The principle of integrated photoelasticity applied to experimental analysis of plates with nonlinear deformations, *Proc. 7-th Intern. Conf. of Experim. Stress Analysis*, Haifa
11. MARKSTRÖM K., STORÄKERS B., 1980, Buckling of cracked members under tension, *Int. J. Solid and Struct.*, **16**, 217-229
12. PATORSKI K., KUJAWIŃSKA M., 1993, *Handbook of the Moiré Fringe Technique*, Elsevier, Amsterdam-London-New York-Tokyo
13. RAKOWSKI G., KACPRZYK Z., 1993, *Metoda elementów skończonych w mechanice konstrukcji*, Oficyna Wydawnicza Politechniki Warszawskiej, Warszawa
14. RAMM E., 1982, *The Riks/Wempner Approach – An Extension of the Displacement Control Method in Nonlinear Analysis*, Pineridge Press, Swensea
15. RIKS E., RANKIN C.C., BROGAN F.A., 1992, The buckling behavior of a central crack in a plate under tension, *Eng. Fract. Mech.*, **43**, 529-547
16. SHAW D., HUANG Y.H., 1990, Buckling behavior of a central cracked thin plate under tension, *Eng. Fract. Mech.*, **35**, 1019-1027
17. SIH G.C., LEE Y.D., 1986, Tensile and compressive buckling of plates weakened by cracks, *Theor. Appl. Fract. Mech.*, **6**, 129-138
18. *Theory and user information*, MSC Marc 2006

Numeryczno-eksperymentalna analiza stanów zakrytycznej deformacji płyty rozciąganej osłabioną szczeliną

Streszczenie

W opracowaniu zaprezentowano metodykę określania rozkładu naprężeń w zakrytycznych stanach deformacji prostokątnej płyty osłabionej szczeliną, poddanej rozciąganiu. Problem został sformułowany jako geometrycznie i fizycznie nieliniowy. Przeprowadzono nieliniową analizę numeryczną w ujęciu metody elementów skończonych. Stany deformacji modelu numerycznego otrzymywane w poszczególnych krokach przyrostowych porównywano z deformacjami określonymi podczas eksperymentu. Uzyskiwane wyniki stanowiły podstawę oceny wpływu rodzaju i wielkości imperfekcji zastosowanych w modelu numerycznym płyty na wiarygodność rezultatów analizy. Rozważano dwa rodzaje imperfekcji: pierwszą – zadaną w formie wstępnej deformacji płyty w strefie szczeliny oraz drugą – polegającą na zastosowaniu zaburzenia w kierunku normalnym do powierzchni środkowej płyty.

Manuscript received February 19, 2009; accepted for print April 16, 2009